

## Hybridization and Spin Decoherence in Heavy-Hole Quantum Dots

Jan Fischer<sup>1,2</sup> and Daniel Loss<sup>1</sup>

<sup>1</sup>*Department of Physics, University of Basel, Klingelbergstrasse 82, CH-4056 Basel, Switzerland*

<sup>2</sup>*Institut für Theoretische Physik, Universität Regensburg, D-93040 Regensburg, Germany*

(Received 29 September 2010; published 22 December 2010)

We theoretically investigate the spin dynamics of a heavy hole confined to an unstrained III-V semiconductor quantum dot and interacting with a narrowed nuclear-spin bath. We show that band hybridization leads to an exponential decay of hole-spin superpositions due to hyperfine-mediated nuclear pair flips, and that the accordant single-hole-spin decoherence time  $T_2$  can be tuned over many orders of magnitude by changing external parameters. In particular, we show that, under experimentally accessible conditions, it is possible to suppress hyperfine-mediated nuclear-pair-flip processes so strongly that hole-spin quantum dots may be operated beyond the “ultimate limitation” set by the hyperfine interaction which is present in other spin-qubit candidate systems.

DOI: [10.1103/PhysRevLett.105.266603](https://doi.org/10.1103/PhysRevLett.105.266603)

PACS numbers: 72.25.Rb, 03.65.Yz, 31.30.Gs, 73.21.La

Heavy holes (HHs) confined to semiconductor quantum dots (QDs) have attracted rapidly growing attention over the last few years for their potential applicability in spintronics and as qubits for quantum information processing devices. The spin states of confined HHs feature very long spin relaxation times [1] and are suspected to be robust against spin decoherence. Typically, for spin qubits operated at sub-Kelvin temperatures, the main source of decoherence is the interaction with the nuclear spins residing in the host material and the inhomogeneous broadening of the nuclear magnetic field (Overhauser field) [2]. For HHs, the form of the nuclear-spin interaction is predominantly Ising-like [3], in contrast to the Heisenberg-type interaction of electrons. Hole-spin QDs in  $p$ -type GaAs/AlGaAs heterostructures have already been realized experimentally and operated in the few-hole regime [4–6]. Experiments in self-assembled InGaAs quantum dots have shown the possibility to initialize and read out the spin state of a HH with high fidelity [7], and ensemble-spin decoherence times  $T_2^*$  on the order of hundreds of nanoseconds have been measured [8].

Several possibilities to suppress decoherence due to inhomogeneous broadening have been proposed, one of which is to prepare the nuclear spins in a so-called narrowed or frequency-focused state [9–11], where the bath is prepared in an eigenstate of the Overhauser operator [see text below Eq. (6)]. On the experimental side, enormous progress has been achieved in preparing such narrowed states [12,13], which have been shown to persist over astonishingly long time scales exceeding hours [13]. For electrons interacting with a narrowed nuclear bath, spin decoherence happens due to nuclear-pair-flip processes induced by the transverse hyperfine interaction, and the associated single-spin decoherence time  $T_2$  can be several orders of magnitude longer than the ensemble-spin decoherence time  $T_2^*$  [14]. For HHs, with their predominantly Ising-like coupling to nuclear spins [3], this transverse

interaction (perpendicular to the Ising axis) can be expected to be very small, potentially leading to very long single-hole-spin decoherence times  $T_2$ .

In this Letter, we study the spin dynamics of a HH confined to a III-V semiconductor QD and interacting with a narrowed nuclear-spin bath. We show that band hybridization leads to non-Ising (transverse) terms in the hyperfine Hamiltonian, whose magnitude depends on the geometry of the QD. This transverse coupling induces nuclear pair-flip processes, leading to fluctuations of the Overhauser field and to exponential single-hole-spin decoherence. We show that for typical unstrained quantum dots the associated time scale  $T_2$  has a lower bound on the order of tens of microseconds and that it can be tuned over many orders of magnitude by changing external parameters such as the applied magnetic field. Thus, it is in principle possible to operate hole-spin QDs in a regime where the hyperfine interaction is practically switched off and where other decoherence mechanisms, such as nuclear dipole or spin-orbit interactions, will become relevant and, hence, experimentally observable.

We start from the  $8 \times 8$  Kane Hamiltonian describing states in the conduction band (CB), heavy-hole (HH), light-hole (LH) and split-off (SO) bands of bulk III-V semiconductors (see Appendix C of Ref. [15]). The Kane Hamiltonian can be “folded down” to an effective  $2 \times 2$  Hamiltonian whose eigenstates describe the spin states in the band of interest, where the admixture of neighboring bands is taken into account perturbatively [15]. Using this procedure, we find the following hybridized HH pseudo-spin states [16]:

$$|\Psi_{\pm}\rangle \approx \mathcal{N}(|u_{\text{HH}}^{\pm}; \phi_{\text{HH}}^{00}\rangle |\pm_{\text{HH}}\rangle \mp \lambda_{\text{CB}} |u_{\text{CB}}^{\pm}; \phi_{\text{CB}}^{0\pm}\rangle |\pm_{\text{CB}}\rangle \pm \lambda_{\text{LH}} |u_{\text{LH}}^{\pm}; \phi_{\text{LH}}^{1\pm}\rangle |\pm_{\text{LH}}\rangle). \quad (1)$$

Here, we have assumed a parabolic confinement potential defining a QD with lateral and perpendicular confinement

lengths  $L$  and  $a_z$ , respectively, and  $\mathcal{N}$  enforces proper normalization of the wave functions. The condition for the validity of Eq. (1) is given by  $a_z \ll L$ , which is needed for the perturbation expansion on the Kane Hamiltonian. The amount of CB and LH admixture is determined by  $\lambda_{\text{CB}} = i\beta_{\text{CB}}P/\sqrt{2}LE_g$  and  $\lambda_{\text{LH}} = \sqrt{3}\beta_{\text{LH}}\gamma_3 a_z L/2\sqrt{2}\gamma_2(L^2 - a_z^2)$ , respectively, where  $P$  is the interband momentum,  $E_g$  is the band gap,  $\gamma_{2,3}$  are Luttinger parameters, and  $\beta_{\text{CB}}, \beta_{\text{LH}}$  account for the difference in effective masses between the bands [16].

Near the  $\Gamma$  point, the spin-orbit-coupled states can be approximated by  $|u_{\text{CB}}^{\pm}\rangle|\pm_{\text{CB}}\rangle \simeq |s\rangle|\uparrow, \downarrow\rangle$ ,  $|u_{\text{HH}}^{\pm}\rangle|\pm_{\text{HH}}\rangle \simeq |p_{\pm}\rangle|\uparrow, \downarrow\rangle$ ,  $|u_{\text{LH}}^{\pm}\rangle|\pm_{\text{LH}}\rangle \simeq (\sqrt{2}|p_z\rangle|\uparrow, \downarrow\rangle \mp |p_{\pm}\rangle|\downarrow, \uparrow\rangle)/\sqrt{3}$ , in terms of  $s$ - and  $p$ -symmetric Bloch states ( $|p_{\pm}\rangle = |p_x\rangle \pm i|p_y\rangle$ ) and real-spin states  $|\uparrow, \downarrow\rangle$  with respect to the growth axis [15]. The envelope functions appearing in Eq. (1) are defined via their position representations  $\langle \mathbf{r}|\phi_{\alpha}^{ij}\rangle = \phi_{\alpha}^{i\perp}(z)\phi_{\alpha}^{j\parallel}(x, y)$  ( $i = 0, 1, j = 0, \pm$ ), where  $\phi_{\alpha}^{\text{0}\parallel}(x, y) = \phi_{\alpha}^0(x)\phi_{\alpha}^0(y)$ ,  $\phi_{\alpha}^{\pm\parallel}(x, y) = [\phi_{\alpha}^1(x)\phi_{\alpha}^0(y) \pm i\phi_{\alpha}^0(x)\phi_{\alpha}^1(y)]/\sqrt{2}$ , and  $\phi_{\alpha}^n(x)$  is the  $n$ th harmonic-oscillator eigenfunction in band  $\alpha$ . Because of terms appearing in the Kane Hamiltonian which are linear in the crystal momentum  $\mathbf{k}$  and which couple neighboring bands, the admixture of CB and LH states features *excited-state* envelope functions. This has profound physical consequences which will be discussed below. The split-off-band contribution to the HH states is very small and has thus been neglected in Eq. (1).

There are three interactions that couple an electron (or HH) to the spins of the surrounding nuclei: the Fermi contact interaction  $h_1^k$ , the anisotropic hyperfine interaction  $h_2^k$ , and the coupling of orbital angular momentum to the nuclear spins  $h_3^k$ , which read (setting  $\hbar = 1$ ) [17]:

$$h_1^k = \frac{\mu_0}{4\pi} \frac{8\pi}{3} \gamma_S \gamma_{j_k} \delta(\mathbf{r}_k) \tilde{\mathbf{S}} \cdot \mathbf{I}_k, \quad (2)$$

$$h_2^k = \frac{\mu_0}{4\pi} \gamma_S \gamma_{j_k} \frac{3(\mathbf{n}_k \cdot \tilde{\mathbf{S}})(\mathbf{n}_k \cdot \mathbf{I}_k) - \tilde{\mathbf{S}} \cdot \mathbf{I}_k}{r_k^3(1 + d/r_k)}, \quad (3)$$

$$h_3^k = \frac{\mu_0}{4\pi} \gamma_S \gamma_{j_k} \frac{\mathbf{L}_k \cdot \mathbf{I}_k}{r_k^3(1 + d/r_k)}. \quad (4)$$

Here,  $\gamma_S = 2\mu_B$ ,  $\gamma_{j_k} = g_{j_k}\mu_N$ ,  $\mu_B$  is the Bohr magneton,  $g_{j_k}$  is the nuclear  $g$  factor of isotopic species  $j_k$  at lattice site  $k$ ,  $\mu_N$  is the nuclear magneton,  $\mathbf{r}_k = \mathbf{r} - \mathbf{R}_k$  is the electron-spin position operator relative to the  $k$ th nucleus with spin  $\mathbf{I}_k$ ,  $d \simeq Z \times 1.5 \times 10^{-15}$  m,  $Z$  is the charge of the nucleus, and  $\mathbf{n}_k = \mathbf{r}_k/r_k$ .  $\tilde{\mathbf{S}}$  and  $\mathbf{L}_k = \mathbf{r}_k \times \mathbf{p}$  denote the spin ( $m_{\tilde{S}} = \pm 1/2$ ) and orbital angular-momentum operators of the electron, respectively.

In order to derive an effective spin Hamiltonian for the HH, we take matrix elements  $\langle \Psi_{\tau} | h_1^k + h_2^k + h_3^k | \Psi_{\tau'} \rangle = H_{\tau\tau'}$  ( $\tau, \tau' = \pm$ ) with respect to the hybridized HH wave functions (1). Because of the  $\delta$  function in Eq. (2), only the

CB admixture contributes to the Fermi contact interaction, since  $p$  states vanish at the positions  $\mathbf{R}_k$  of the nuclei. On the other hand, the terms in Eq. (1) associated with HH and LH states contribute to matrix elements of Eqs. (3) and (4), while the CB admixture does not contribute due to symmetry ( $h_2^k$ ) and vanishing orbital angular momentum ( $h_3^k$ ). Adding up all contributions, and taking into account a Zeeman term due to a magnetic field  $B$  along the  $z$  direction, we find the following effective spin Hamiltonian describing the hole-nuclear-spin interactions:

$$H = (b + h^z)S^z + \frac{1}{2}(h^+S^- + h^-S^+). \quad (5)$$

Here,  $b = g_h\mu_B B$  is the Zeeman energy of the HH,  $g_h \simeq 2$  is the HH  $g$  factor along the magnetic-field direction  $z$ ,  $\mu_B$  is the Bohr magneton, and  $\mathbf{S}$  is the HH pseudospin-1/2 operator. The Overhauser-field components are defined by  $h^z = \sum_k A_k^z I_k^z$  and  $h^{\pm} = \sum_k A_k^{\pm} I_k^{\pm}$  ( $I_k^{\pm} = I_k^x \pm iI_k^y$ ), where  $A_k^z$  and  $A_k^{\pm}$  denote the longitudinal and transverse hyperfine coupling of the HH to the  $k$ th nuclear spin, respectively. The flip-flop terms in Eq. (5) couple the HH pseudospin ( $\pm 3/2$ ) states through admixture with CB and LH pseudospin ( $\pm 1/2$ ) states, such that flip-flop processes with  $I = 1/2$  nuclear spins preserve the total angular momentum.

The hybridized states in Eq. (1) are predominantly HH-like. In Ref. [3] it has been shown that taking matrix elements of the Hamiltonians (2)–(4) with respect to pure HH states (i.e., neglecting band hybridization) results in an Ising Hamiltonian  $h^z S^z$ . The longitudinal coupling constants are thus dominated by the HH contribution,  $A_k^z \simeq A_{k,\text{HH}}^z$ , and the transverse (non-Ising) terms in Eq. (5) are only due to hybridization with CB and LH states,  $A_k^{\pm} = A_{k,\text{CB}}^{\pm} + A_{k,\text{LH}}^{\pm}$ . Explicitly, the longitudinal and transverse coupling constants are given by  $A_{k,\text{HH}}^z \simeq A_{\text{HH}}^j v_0 |\phi_0(z_k)|^2 |\phi_0(x_k, y_k)|^2$ ,  $A_{k,\text{CB}}^{\pm} \simeq A_{\text{CB}}^j v_0 |\phi_0(z_k)|^2 \phi_{\pm}^*(x_k, y_k) \phi_{\mp}(x_k, y_k)$ , and  $A_{k,\text{LH}}^{\pm} \simeq A_{\text{LH}}^j v_0 |\phi_1(z_k)|^2 \phi_{\mp}^*(x_k, y_k) \phi_{\pm}(x_k, y_k)$ , respectively, where  $v_0$  is the volume occupied by one nucleus and  $A_{\alpha}^j$  is the hyperfine coupling strength of isotope  $j$  associated with band  $\alpha$ . Introducing the average  $A_{\alpha} = \sum_j v_j A_{\alpha}^j$ , where  $v_j$  denotes the abundance of isotope  $j$ , we estimate  $A_{\text{HH}} \simeq -13 \mu\text{eV}$  [3],  $A_{\text{CB}} \simeq 0.15 \mu\text{eV}$ , and  $A_{\text{LH}} \simeq 0.05 \mu\text{eV}$  for a GaAs QD with  $L = 10$  nm and  $a_z = 2$  nm. In contrast to the interaction of an electron with nuclear spins, the hole-nuclear-spin interaction given in Eq. (5) is highly anisotropic.

We now study the dynamics of the transverse spin component  $S^+$  describing the coherence of the HH pseudospin states. To this end, we use the Nakajima-Zwanzig master equation [9]

$$\langle \dot{S}^+ \rangle_t = i\omega_n \langle S^+ \rangle_t - i \int_0^t dt' \Sigma(t-t') \langle S^+ \rangle_{t'}, \quad (6)$$

where  $\omega = b + h^z$ ,  $\omega|n\rangle = \omega_n|n\rangle$ , and  $|n\rangle$  denotes a narrowed state of the nuclear-spin system (note that for a

non-narrowed bath, the HH decoherence would be dominated by the Ising part of Eq. (5), as shown in Ref. [3].  $\Sigma(t) = \text{tr}\{S^+ \hat{\Sigma}(t) S^- |n\rangle\langle n|\}$  is the self-energy (or memory kernel) describing the transverse-spin dynamics, where  $\hat{\Sigma}(t) = -iPLQe^{iLQ}QLP$ ,  $P$  is a projector onto a product state of HH and nuclear spins,  $Q = 1 - P$ , and  $LQ = [H, Q]$  for some operator  $Q$  acting on the total Hilbert space of HH and nuclear spins [9]. It is convenient to perform a Laplace transform on Eq. (6), yielding an algebraic equation of the form

$$S^+(s + i\omega_n) = \frac{\langle S^+ \rangle_0}{s + i\Sigma(s + i\omega_n)} \quad (7)$$

in the frame rotating with frequency  $\omega_n$ . Equations (6) and (7) are exact equations describing, in general, non-Markovian dynamics of the transverse HH-spin component. The structure of the self-energy  $\Sigma(s)$  is, however, very complex, so we have to resort to an approximation scheme. The energy scales associated with the transverse coupling  $V = (h^+ S^- + h^- S^+)/2$  are much smaller than those associated with the longitudinal coupling  $H_0 = (b + h^z)S^z$  (see above), and we expand the self-energy in powers of hole-nuclear-spin flip-flop processes induced by  $V$ :  $\Sigma(s) = \Sigma^{(2)}(s) + \Sigma^{(4)}(s) + \mathcal{O}(V^6)$ . Odd orders in  $V$  vanish because of the Zeeman mismatch between HH and nuclear spins which energetically forbids such processes. For a nuclear spin  $I$  of order unity, the smallness parameter which controls this expansion is given approximately by  $A_\perp/\omega_n$  (see Appendix A of Ref. [9]), where  $A_\perp = \sqrt{A_{\text{CB}}^2 + A_{\text{LH}}^2}$ .

We evaluate the second- and fourth-order self-energy contributions explicitly, following the procedure described in Ref. [18]. We find, for a homonuclear system in the frame rotating with frequency  $\omega_n$ ,

$$\Sigma^{(2)}(s + i\omega_n) \simeq -\frac{c_+ + c_-}{4\omega_n} \sum_k |A_k^\pm|^2, \quad (8)$$

$$\Sigma^{(4)}(s + i\omega_n) \simeq -i \frac{c_+ c_-}{4\omega_n^2} \sum_{k_1, k_2} \frac{|A_{k_1}^\pm|^2 |A_{k_2}^\pm|^2}{s + i(A_{k_1}^z - A_{k_2}^z)}, \quad (9)$$

where the sums run over all nuclear sites  $k$ . We have introduced  $c_\pm = I(I+1) - \langle\langle m(m \pm 1) \rangle\rangle$ , where  $I$  is the nuclear spin,  $m = -I, \dots, I$ , and the double angle bracket indicates averaging over the  $I_k^z$  eigenvalues  $m$  [9].

We emphasize that the structure of the self-energies  $\Sigma^{(2)}$  and  $\Sigma^{(4)}$  bears some similarity with previous results on electron-spin decoherence [18]. However, there are two important differences compared to the electron case: (i) The appearance of different coupling constants  $A_k^z$  and  $A_k^\pm$  in Eqs. (8) and (9) is due to the anisotropy of the hyperfine Hamiltonian (5) and provides an additional smallness factor  $A_\perp/A_z \ll 1$  ( $A_z = |A_{\text{HH}}|$ ) to the self-energy (11); (ii) the spatial dependence of the transverse coupling constants differs from the longitudinal ones due

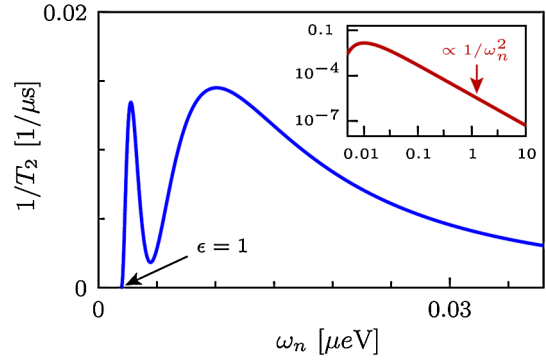


FIG. 1 (color online). Decoherence rate  $1/T_2$  from Eq. (12) as a function of the HH Zeeman energy  $\omega_n = g_h \mu_B B + p I A_{\text{HH}}$ . For  $L = 10$  nm and  $a_z = 4$  nm, we estimate  $N \simeq 7.3 \times 10^4$ . Inset:  $1/T_2$  for fields up to 1 T (axes in the same units as in the main figure).

to the appearance of excited-state envelope functions. In particular, this means that nuclear spins at the edge of the QD (rather than in its center as in the electron case) couple most strongly to the HH along the transverse direction—an effect which manifests itself directly in the appearance of a distinct minimum in the decoherence rate  $1/T_2$  (see Fig. 1).

We now evaluate the second- and fourth-order self-energy in the continuum limit (changing sums to integrals [16]), following Ref. [18]. Since  $a_z \ll L$  (see above), we can perform a two-dimensional limit by averaging over the  $z$  dependence in the hyperfine coupling constants  $A_k^z$  and  $A_k^\pm$ . From Eq. (8), we see that the second-order self-energy  $\Sigma^{(2)}$  is purely real, leading to no decay but a frequency shift  $\Delta\omega = -\text{Re}\Sigma^{(2)}(s + i\omega_n)$ , or

$$\Delta\omega = \frac{c_+ + c_-}{16N} \frac{A_\perp^2}{\omega_n}, \quad (10)$$

where  $N$  is the number of nuclear spins enclosed by the envelope function. The fourth-order self-energy becomes

$$\Sigma^{(4)}(s + i\omega_n) \simeq -i \frac{c_+ c_-}{4N} \frac{A_\perp}{A_z} \frac{A_\perp^3}{\omega_n^2} \times \int_0^1 dx \int_0^1 dy \frac{x(\log x)^2 y(\log y)^2}{s + i(x - y)} \quad (11)$$

in the continuum limit, where  $x = \exp\{-r_1^2\}$ ,  $y = \exp\{-r_2^2\}$ , and  $r_i = \sqrt{x_i^2 + y_i^2}/L$  ( $i = 1, 2$ ). Here, we have approximated  $|A_k^\pm|^2 \simeq |A_{k,\text{CB}}^\pm|^2 + |A_{k,\text{LH}}^\pm|^2$  since the overlap term vanishes under spatial averaging. The appearance of polynomial prefactors  $r^4$ , represented by the log functions in the numerator of Eq. (11), is a direct consequence of the excited-state envelope functions describing the distribution of transverse coupling constants  $A_k^\pm$  within the quantum dot.

The transverse-spin dynamics of the HH are described by the nonanalytic structure of the right-hand side of

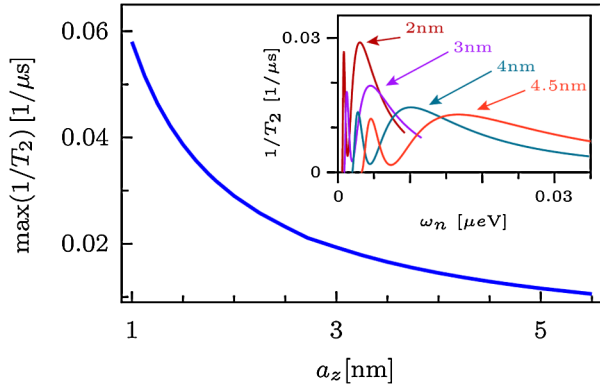


FIG. 2 (color online). Maximum of the decoherence rate  $1/T_2$  as a function of the QD height  $a_z$ . For increasing  $a_z$ , the maximal value of  $1/T_2$  decreases (see main plot) and the position of the maximum is shifted (see inset).

Eq. (7) (see, e.g., Ref. [18]). Inserting  $\Sigma^{(2)}$  and  $\Sigma^{(4)}$  into Eq. (7), we find one pole at  $s \approx i\Delta\omega - \Gamma$ , whose negative real part gives the HH decoherence rate  $\Gamma = 1/T_2 \approx -\text{Im}\Sigma^{(4)}(i\omega_n + i\Delta\omega - 0^+)$  [18], where  $0^+$  denotes a positive infinitesimal. Evaluating Eq. (11), we find [16]

$$\frac{1}{T_2} = \frac{\pi c_+ c_-}{4N} \frac{A_\perp}{A_z} \frac{A_\perp^3}{\omega_n^2} \int_\epsilon^1 dx x [\log x]^2 (x + \epsilon) [\log(x + \epsilon)]^2, \quad (12)$$

where  $\epsilon = N|\Delta\omega/A_{\text{HH}}|$ . The integral in Eq. (12) can now be evaluated numerically for any value of  $\epsilon$ .

The Zeeman energy of the HH is given by  $\omega_n = g_n \mu_B B + p I A_{\text{HH}}$ , where  $-1 \leq p \leq 1$  is the degree of nuclear-spin polarization (along the positive  $z$  direction). In Fig. 1, we show the hole-spin decoherence rate  $1/T_2$  as a function of  $\omega_n$ . The nonmonotonic behavior of  $1/T_2$  for small  $\omega_n$  appears when  $\epsilon \propto 1/\omega_n$  approaches unity.

For electrons, a nonmonotonic behavior of  $1/T_2$  has been predicted as well [18], albeit with a different dependence on  $\epsilon$  and around magnetic fields of several Tesla. In contrast, for holes, the nonmonotonicity occurs at much lower fields ( $B \approx 0.1$  mT for the parameters used in Fig. 1 assuming  $p = 0$ ), and the rate  $1/T_2$  features an additional dip which is a footprint of the excited-state envelope functions appearing in Eq. (1). The huge difference in energy scales has very important consequences for the tunability of the hole-spin decoherence rate: by increasing the externally applied magnetic field (or the degree of nuclear-spin polarization), it is possible to decrease  $1/T_2$  over many orders of magnitude within the experimentally accessible range of magnetic fields (see inset of Fig. 1). This means that this system offers the possibility to entirely “turn off” hyperfine-associated spin decoherence. As a consequence, hole-spin quantum dots may be operated in a regime where other interactions, such as spin-orbit or direct nuclear dipole interactions, will be the dominant source of spin decoherence and will therefore become

experimentally observable. On the other hand, for small  $\omega_n$ , the hybridization-induced transverse interaction can be expected to be the dominant source of hole-spin decoherence. We emphasize that Eq. (12) is still valid at  $B = 0$ , as long as  $\epsilon < 1$ . For  $\epsilon > 1$ ,  $\Delta\omega$  exceeds the bandwidth of excitations  $A_z/N$  in the nuclear bath, and the perturbation expansion breaks down [18].

The degree of band hybridization, and therefore the decoherence rate  $1/T_2$ , depends on the geometry of the QD, i.e., on  $L$  and  $a_z$ . For flat QDs the amount of LH admixture to the HH states (1) is decreased, leading to smaller non-Ising terms in the Hamiltonian (5). On the other hand, the envelope wave function of a flat dot encloses less nuclear spins (for fixed  $L$ ). These two effects lead to an increase of the maximal decoherence rate for smaller  $a_z$  (see Fig. 2), and a shift of its position as a function of  $\omega_n$  (see inset of Fig. 2).

We acknowledge discussions with B. Braunecker, W. A. Coish, F. Pedrocchi, D. Stepanenko, and M. Trif, and funding from the Swiss NSF, NCCR Nanoscience, and DARPA Quest.

- 
- [1] D. V. Bulaev and D. Loss, *Phys. Rev. Lett.* **95**, 076805 (2005); D. Heiss *et al.*, *Phys. Rev. B* **76**, 241306 (2007); M. Trif, P. Simon, and D. Loss, *Phys. Rev. Lett.* **103**, 106601 (2009).
  - [2] J. R. Petta *et al.*, *Science* **309**, 2180 (2005).
  - [3] J. Fischer *et al.*, *Phys. Rev. B* **78**, 155329 (2008).
  - [4] Y. Komijani *et al.*, *Europhys. Lett.* **84**, 57004 (2008).
  - [5] M. Csontos *et al.*, *Appl. Phys. Lett.* **97**, 022110 (2010).
  - [6] O. Klochan *et al.*, *Appl. Phys. Lett.* **96**, 092103 (2010).
  - [7] B. D. Gerardot *et al.*, *Nature (London)* **451**, 441 (2008).
  - [8] D. Brunner *et al.*, *Science* **325**, 70 (2009).
  - [9] W. A. Coish and D. Loss, *Phys. Rev. B* **70**, 195340 (2004).
  - [10] D. Klauser, W. A. Coish, and D. Loss, *Phys. Rev. B* **73**, 205302 (2006).
  - [11] D. Stepanenko *et al.*, *Phys. Rev. Lett.* **96**, 136401 (2006).
  - [12] A. Greilich *et al.*, *Science* **313**, 341 (2006); D. J. Reilly *et al.*, *Science* **321**, 817 (2008); A. Greilich *et al.*, *Nature Phys.* **5**, 262 (2009); C. Latta *et al.*, *Nature Phys.* **5**, 758 (2009); X. Xu *et al.*, *Nature (London)* **459**, 1105 (2009); I. T. Vink *et al.*, *Nature Phys.* **5**, 764 (2009); H. Bluhm *et al.*, *Phys. Rev. Lett.* **105**, 216803 (2010).
  - [13] A. Greilich *et al.*, *Science* **317**, 1896 (2007).
  - [14] W. A. Coish, J. Fischer, and D. Loss, *Phys. Rev. B* **77**, 125329 (2008); Ł. Cywiński, W. M. Witzel, and S. Das Sarma, *Phys. Rev. B* **79**, 245314 (2009).
  - [15] R. Winkler, *Spin-Orbit Coupling Effects in Two-Dimensional Electron and Hole Systems*, Springer Tracts in Modern Physics, Vol. 191 (Springer-Verlag, Berlin, 2003).
  - [16] See supplementary material at <http://link.aps.org/supplemental/10.1103/PhysRevLett.105.266603>.
  - [17] A. M. Stoneham, *Theory of Defects in Solids* (Oxford University Press, New York, 1972), Chap. 13.
  - [18] W. A. Coish, J. Fischer, and D. Loss, *Phys. Rev. B* **81**, 165315 (2010).